13th World Conference on Earthquake Engineering
Vancouver, B.C., Canada
August 1-6, 2004
Paper No. 530

COMPUTATIONAL MODELING OF NONLINEAR SOIL-STRUCTURE INTERACTION ON PARALLEL COMPUTERS

Jinchi LU[1], Zhaohui YANG[2], Liangcai HE[3], Jun PENG[4], Ahmed ELGAMAL[5], and Kincho H. LAW[6]

SUMMARY

In order to satisfactorily reproduce the Soil-Structure Interaction (SSI) effects under earthquake loading, it is often necessary to model a large domain of the soil surrounding the structure of interest. High spatial/temporal resolution is another challenge in analyzing these models. A new parallel nonlinear finite element program, ParCYCLIC, is employed to study such high fidelity large-scale SSI models. ParCYCLIC incorporates a constitutive model that has been calibrated by physical tests to represent the salient characteristics of sand liquefaction and associated accumulation of shear deformations. The numerical implementation is designed for distributed-memory parallel computer systems, and allows for performing explicit as well as implicit time integration. In this paper, a single pile embedded in mildly inclined, liquefiable soil deposit is analyzed under dynamic base shaking conditions. Aspects of model response, including pore pressure generation/dissipation, soil lateral deformation during liquefaction, and pile displacement and bending moment, are presented and discussed.

INTRODUCTION

Liquefaction and associated shear deformation is a major cause of earthquake-related damage to piles and pile-supported structures. Pile foundation damage due to lateral spreading induced by liquefaction is documented in numerous reports and papers [1-3].

The recognition of the importance of lateral ground displacement on pile performance has led to the development of analytical models capable of evaluating the associated potential problems [4]. Modeling lateral ground displacement and pile response involves complex aspects of SSI mechanisms. In addition, computational models of ground response under earthquake loading conditions may require a high level

[1] Ph.D. Candidate, University of California, San Diego, La Jolla, USA. Email: jinlu@ucsd.edu
[2] Assistant Research Scientist, University of California, San Diego, La Jolla, USA. Email: zhyang@ucsd.edu
[3] Ph.D. Candidate, University of California, San Diego, La Jolla, USA. Email: lhe@ucsd.edu
[4] Research Associate, Stanford University, Stanford, USA. Email: junpeng@stanford.edu
[5] Professor, University of California, San Diego, La Jolla, USA. Email: elgamal@ucsd.edu
[6] Professor, Stanford University, Stanford, USA. Email: law@stanford.edu

of spatial resolution. A large domain of the ground surrounding the super-structure may be necessary in order to satisfactorily represent the involved SSI mechanisms.

A new parallel nonlinear finite element program, ParCYCLIC, recently developed on distributed memory parallel computers, is employed to study such high fidelity large-scale SSI models. ParCYCLIC, is implemented based on a serial program CYCLIC, which is a nonlinear finite element program developed to analyze liquefaction-induced seismic response [5,6]. Extensive calibration of CYCLIC has been conducted with results from experiments and full-scale response of earthquake simulations involving ground liquefaction [7]. In ParCYCLIC, the calibrated serial code for modeling of earthquake geotechnical phenomena is combined with advanced computational methodologies to facilitate the simulation of large-scale systems and broaden the scope of practical applications.

This paper presents a pilot three-dimensional (3D) Finite Element study of dynamic pile response in liquefied sloping ground. The numerical simulation was conducted using ParCYCLIC on the AMD Cluster parallel computer at the University of Michigan.

PARALLEL FINITE ELEMENT PROGRAM

Finite Element Formulation

In ParCYCLIC, the saturated soil system is modeled as a two-phase material based on the Biot [8] theory for porous media. A numerical framework of this theory, known as *u-p* formulation, was implemented [5,6,9]. In the *u-p* formulation, displacement of the soil skeleton *u*, and pore pressure *p*, are the primary unknowns [10,11]. The implementation of ParCYLCIC is based on the following assumptions: small deformation and rotation, constant density of the solid and fluid in both time and space, locally homogeneous porosity which is constant with time, incompressibility of the soil grains, and equal accelerations for the solid and fluid phases.

The *u-p* formulation as defined by Chan [10] consists of: i) equation of motion for the solid-fluid mixture, and ii) equation of mass conservation for the fluid phase, incorporating equation of motion for the fluid phase and Darcy's law. The finite element governing equations can be expressed in matrix form as follows [10]:

$$\mathbf{M}\ddot{\mathbf{U}} + \int_{\Omega} \mathbf{B}^{\mathrm{T}} \boldsymbol{\sigma}' \, d\Omega + \mathbf{Q}\mathbf{p} - \mathbf{f}^{s} = \mathbf{0} \qquad (1a)$$

$$\mathbf{Q}^{\mathrm{T}}\dot{\mathbf{U}} + \mathbf{S}\dot{\mathbf{p}} + \mathbf{H}\mathbf{p} - \mathbf{f}^{p} = \mathbf{0} \qquad (1b)$$

where **M** is the mass matrix, **U** the displacement vector, **B** the strain-displacement matrix, $\boldsymbol{\sigma}'$ the effective stress tensor (determined by the soil constitutive model described below), **Q** the discrete gradient operator coupling the solid and fluid phases, **p** the pore pressure vector, **S** the compressibility matrix, and **H** the permeability matrix. The vectors $\mathbf{f}^{s}$ and $\mathbf{f}^{p}$ represent the effects of body forces and prescribed boundary conditions for the solid-fluid mixture and the fluid phase respectively.

In eq. 1a (equation of motion), the first term represents inertia force of the solid-fluid mixture, followed by internal force due to soil skeleton deformation, and internal force induced by pore-fluid pressure. In eq. 1b (equation of mass conservation), the first two terms represent the rate of volume change for the soil skeleton and the fluid phase respectively, followed by the seepage rate of the pore fluid. Eqs. 1a and 1b are integrated in time using a single-step predictor multi-corrector scheme of the Newmark type [10,12]. In the current implementation, the solution is obtained for each time step using the modified Newton-Raphson approach [6].

Soil Constitutive Model

The second term in eq. 1a is defined by the soil stress-strain constitutive model. The finite element program incorporates a soil constitutive model [5,6,13,14] based on the original multi-surface-plasticity theory for frictional cohesionless soils [15]. This model was developed with emphasis on simulating the liquefaction-induced shear strain accumulation mechanism in clean cohesionless soils [5,7,13,14,16]. Special attention was given to the deviatoric-volumetric strain coupling (dilatancy) under cyclic loading, which causes increased shear stiffness and strength at large cyclic shear strain excursions (i.e., cyclic mobility).

The constitutive equation is written in incremental form as follows [15]:

$$\dot{\boldsymbol{\sigma}}' = \boldsymbol{E} : (\dot{\boldsymbol{\varepsilon}} - \dot{\boldsymbol{\varepsilon}}^{p}) \tag{2}$$

where $\dot{\boldsymbol{\sigma}}'$ is the rate of effective Cauchy stress tensor, $\dot{\boldsymbol{\varepsilon}}$ the rate of deformation tensor, $\dot{\boldsymbol{\varepsilon}}^{p}$ the plastic rate of deformation tensor, and $\boldsymbol{E}$ the isotropic fourth-order tensor of elastic coefficients. The rate of plastic deformation tensor is defined by: $\dot{\boldsymbol{\varepsilon}}^{p} = \mathbf{P} \langle L \rangle$, where $\mathbf{P}$ is a symmetric second-order tensor defining the direction of plastic deformation in stress space, L the plastic loading function, and the symbol $\langle\ \rangle$ denotes the McCauley's brackets (i.e., $\langle L \rangle = \max(L, 0)$). The loading function L is defined as: $L = \mathbf{Q} : \dot{\boldsymbol{\sigma}}' / H'$ where H' is the plastic modulus, and $\mathbf{Q}$ a unit symmetric second-order tensor defining yield-surface normal at the stress point (i.e., $\mathbf{Q} = \nabla f / \|\nabla f\|$), with the yield function f selected of the following form [13]:

$$f = \frac{3}{2}(\boldsymbol{s} - (p' + p_0')\boldsymbol{\alpha}) : (\boldsymbol{s} - (p' + p_0')\boldsymbol{\alpha}) - M^2 (p' + p_0')^2 = 0 \tag{3}$$

in the domain of $p' \geq 0$. The yield surfaces in principal stress space and deviatoric plane are shown in Fig. 1. In eq. 3, $\boldsymbol{s} = \boldsymbol{\sigma}' - p' \boldsymbol{\delta}$ is the deviatoric stress tensor, p' the mean effective stress, p_0' a small positive constant (1.0 kPa in this paper) such that the yield surface size remains finite at $p' = 0$ for numerical convenience (Fig. 1), $\boldsymbol{\alpha}$ a second-order kinematic deviatoric tensor defining the surface coordinates, and M dictates the surface size. In the context of multi-surface plasticity, a number of similar surfaces with a common apex form the hardening zone (Fig. 1). Each surface is associated with a constant plastic modulus. Conventionally, the low-strain (elastic) moduli and plastic moduli are postulated to increase in proportion to the square root of p' [15].

The flow rule is chosen so that the deviatoric component of flow $\mathbf{P}' = \mathbf{Q}'$ (associative flow rule in the deviatoric plane), and the volumetric component P'' defines the desired amount of dilation or contraction in accordance with experimental observations. Consequently, P'' defines the degree of non-associativity of the flow rule and is given by [6]:

$$P'' = \frac{(\eta / \overline{\eta})^2 - 1}{(\eta / \overline{\eta})^2 + 1} \Psi \tag{4}$$

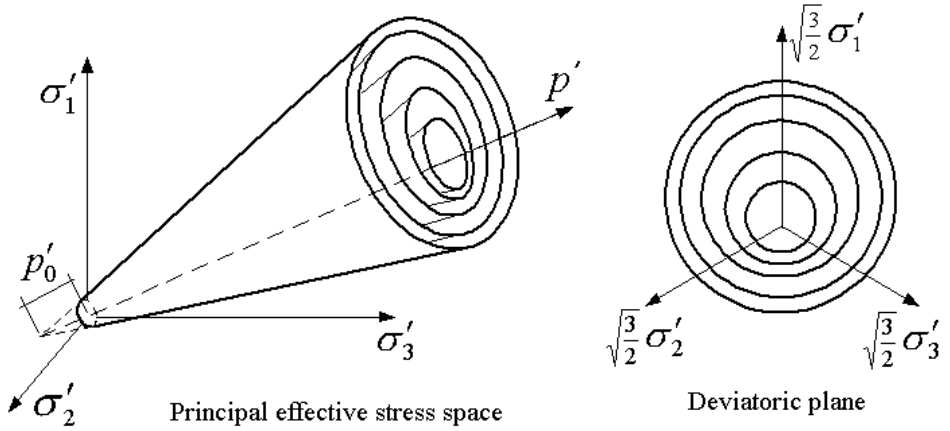

Fig. 1: Conical yield surfaces for granular soils in principal stress space and deviatoric plane [9,12,15,17]

where $\eta = ((3/2)\boldsymbol{s} : \boldsymbol{s})^{1/2} / p'$ is effective stress ratio, $\overline{\eta}$ a material parameter defining the stress ratio along the phase transformation (PT) surface [18], and Ψ a scalar function controlling the amount of dilation or contraction depending on the level of confinement and/or cumulated plastic deformation [13].

The employed model has been extensively calibrated for clean Nevada Sand at $D_r \approx 40\%$ [6,9]. Calibration was based on results of monotonic and cyclic laboratory tests [19], as well as data from level-ground and mildly inclined infinite-slope dynamic centrifuge-model simulations [20,21]. The main modeling parameters include standard dynamic soil properties such as low-strain shear modulus and friction angle, as well as calibration constants to control the dilatancy effects (phase transformation angle, contraction and dilation parameters), and the level of liquefaction-induced yield strain.

Parallel Implementation

Parallel program strategies

Programming architectures required to take advantage of parallel computers are significantly different from the traditional paradigm for a serial program [22]. In a parallel computing environment, care must be taken to maintain all participating processors busy performing useful computations and to minimize communication among the processors. ParCYCLIC employs the single-program-multiple-data (SPMD) paradigm, a common approach in developing application software for distributed memory parallel computes. In this approach, problems are decomposed using well-known domain decomposition techniques. Each processor of the parallel machine solves a partitioned domain, and data communications among sub-domains are performed through message passing. The domain decomposition method (DDM) is attractive in parallel finite element computations because it allows individual sub-domain operations to be performed concurrently on separate processors. The SPMD model has been applied successfully in the development of many parallel finite element programs from legacy serial code [23,24].

Parallel Sparse Solver

Nonlinear finite element computations of earthquake simulations involve the iterative solution of sparse symmetric systems of linear equations. Solving the linear system is often the most computationally intensive task, especially when an implicit time integration scheme is employed. ParCYCLIC employs a direct sparse solution method proposed and developed by Law and Mackay [25]. The parallel sparse

solver is based on a row-oriented storage scheme that takes full advantage of the sparsity of the stiffness matrix. The concept of the sparse solver incorporated in ParCYCLIC is briefly described below.

Given a linear system of equations $Kx = f$, the symmetric sparse matrix K is often factored into the matrix product LDL^T, where L is a lower triangular matrix and D is a diagonal matrix. The solution vector x is then computed by a forward solution, $Lz = f$ or $z = L^{-1}f$, followed by a backward substitution $DL^Tx = z$ or $x = L^{-T}D^{-1}z$. Sparse matrix factorization can be divided into two phases: symbolic factorization and numeric factorization [25]. Symbolic factorization determines the structure of matrix factor L from that of K (i.e. locations of nonzero entries). Numeric factorization then makes use of the data structure determined to compute the numeric values of L and D. The nonzero entries in L can be determined by the original nonzero entries of K and a list vector, which is defined as:

$$PARENT(j) = \min\{i \mid L_{ij} \neq 0\} \qquad (4)$$

in which j is the column number and i the row subscript. The array *PARENT* represents the row subscript of the first nonzero entry in each column of the lower matrix factor L. The definition of the array *PARENT* results in a monotonically ordered elimination tree T of which each node has its numbering higher than its descendants [26]. The list array *PARENT* contains sufficient information for determining the nonzero structure of any row in L. Furthermore, by topologically postordering the elimination tree, the nodes in any subtree can be numbered consecutively [27]. The resulting sparse matrix factor is partitioned into block submatrices where the columns/rows of each block correspond to the node set of a branch in T. Fig. 2 shows a simple finite element grid and its post-ordered elimination tree representation.

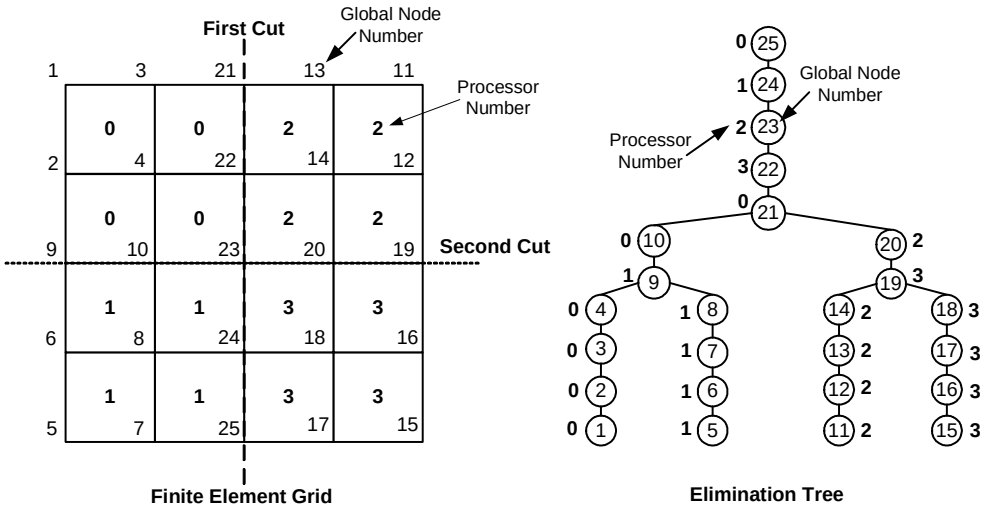

Fig. 2: A finite element mesh and its elimination tree representation[28-30]

For parallel implementation of the sparse matrix factorization, the processor assignment strategy can be based on matrix partitioning according to the post-ordered elimination tree. The coefficients of a sparse matrix factor are distributively stored among the processors according to the column blocks. Essentially, the strategy is to assign the rows corresponding to the nodes along each branch (column block) of the elimination tree to a processor or a group of processors. Beginning at the root of the elimination tree, the nodes belonging to this branch of the tree are assigned among the available processors in a rotating round robin fashion. As we traverse down the elimination tree, at each fork of the elimination tree, the group of processors is divided to match the number and the size of the subtrees below the current branch. A separate group of processors is assigned to each branch at the fork and the process is repeated for each subtree.

The parallel numerical factorization procedure is divided into two phases [25]. In the first phase, each processor independently factorizes certain portions of the matrix assigned to a single processor. In the second phase, other portions of the matrix shared by more than one processor are factored. Following the parallel factorization, the parallel forward and backward solution phases proceed to compute the solution to the global system of equations.

SIMULATION OF SOIL-PILE INTERACTION IN LIQUEFIED SLOPING GROUND

In this section, numerical simulation of the response of a single-pile foundation in a liquefied ground (Fig. 3) is presented. The soil profile consists of a saturated loose liquefiable sand layer (relative density D_r = 40%, 6m in thickness), underlain by a slightly cemented non-liquefiable sand layer (2m thick) [31]. The single pile (square in cross section) is 0.6m in width, 8m in length, has a bending stiffness, EI = 8000 kN/m^2, and is free at the top. The bedrock base underneath the soil strata has an inclination angle of 4°. The single pile foundation is subjected to a predominantly 2Hz harmonic base excitation with a peak acceleration of about 0.2g.

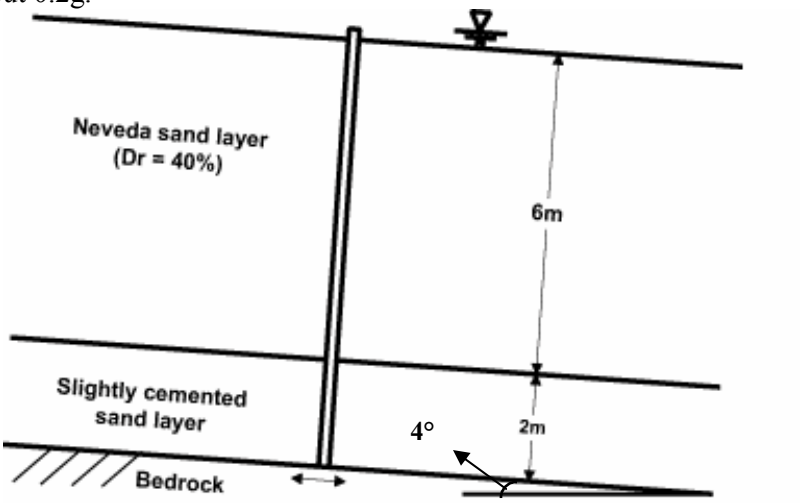

Fig. 3: A single pile foundation in a slightly sloping ground

Numerical Modeling

The single pile foundation was simulated using the above-described three-dimensional parallel finite element program ParCYCLIC. A 30m by 16m of soil domain surrounding the pile was considered. As shown in Fig. 4, the soil domain and the single pile were discretized using 3D 8-node brick elements. A total of 13,824 3D brick elements constitute the FE mesh. A half mesh configuration is used due to geometrical symmetry. The boundary conditions were (i) lateral excitation was defined along the longitudinal direction of the base (Fig. 4b), (ii) at any given depth, displacement degrees of freedom of the downslope and upslope boundaries were tied together (both horizontally and vertically using the penalty method) to reproduce a 1D shear beam effect [6], (iii) the soil surface was traction free, with zero prescribed pore pressure, and (iv) the base and lateral boundaries were impervious.

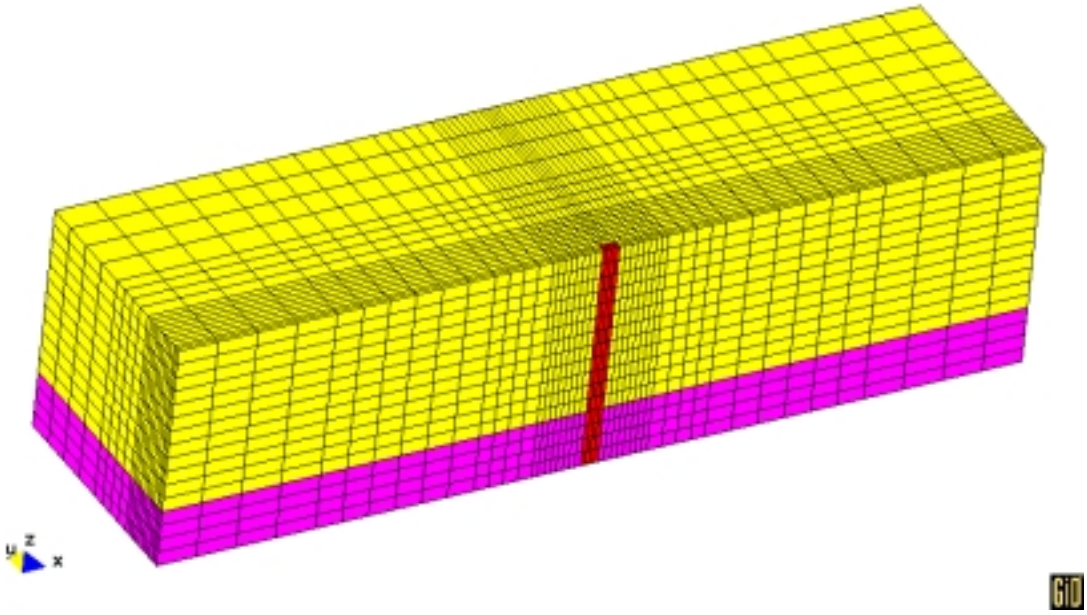

(a) Finite element mesh

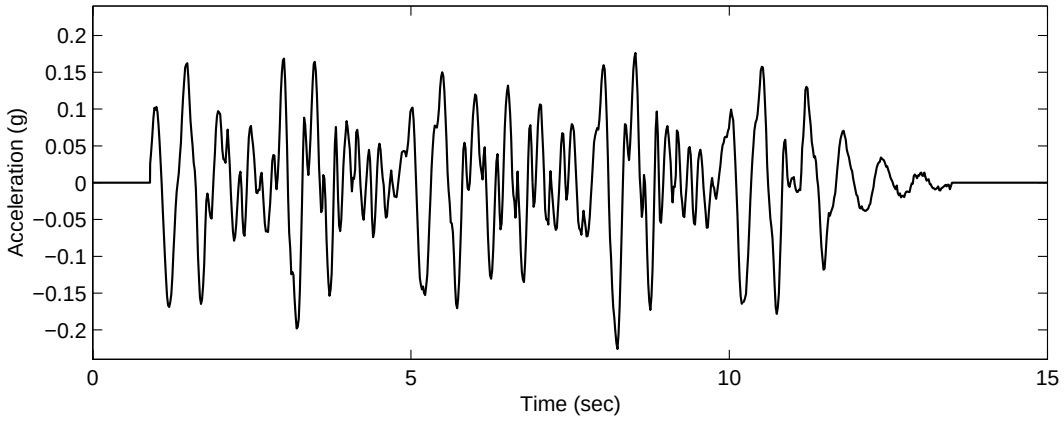

(b) Input motion

Fig. 4: Finite element mesh and input motion

A static application of gravity (model own weight) was performed before seismic excitation. The resulting fluid hydrostatic pressures and soil stress-states served as initial conditions for the subsequent dynamic analysis [7].

A total 5000 time steps of analysis was performed at 0.01 second per step. The run was conducted on the AMD Cluster at the Center for Advanced Computing (CAC), University of Michigan. The AMD Cluster has 128 nodes of dual Athlon 2000MP CPUs and each node has 2 CPUs and 2 GB of RAM. The total wall-clock execution time for the simulation was approximately 20 hours using 8 processors.

.

Computation Results and Discussion

Acceleration and Pore Pressure in Soil

Figs. 5-6 display the computed lateral accelerations and pore pressure time histories along the model depth. Initially, the input motion was amplified near ground surface. After about 4 seconds of shaking,

de-amplification occurred from surface down to 2m depth (Fig. 5), as this portion of the soil domain reached liquefaction (Fig. 6), indicated by the pore-pressure ratio r_u approaching 1.0 ($r_u = u_e/\sigma_v'$ where u_e is excess pore pressure, and σ_v' initial effective vertical stress).

The top portion of the loose sand layer remained liquefied until the end of shaking and beyond. Thereafter, excess pore pressure started to dissipate. The computed excess pore pressure time histories displayed a number of instantaneous sharp pore pressure drops after initial liquefaction (Fig. 6). These drops coincided with the acceleration spikes that occurred exclusively in the negative direction (Fig. 5).

Soil and Pile Lateral Displacement

The mild inclination imposed a static shear stress component (due to gravity), causing accumulated cycle-by-cycle lateral deformation (Fig. 7). The permanent lateral displacement of the ground surface after shaking is approximately 45cm. All lateral displacements occurred in the top 6.0m within the liquefiable sand layer. The top graph of Fig. 7 shows pile head lateral displacement during and after shaking. The final lateral displacement of pile head is approximately 17cm.

Fig. 8 shows the profiles of pile and free-field soil lateral displacement at different time instants during the shaking (5 and 10 seconds) as well as after the shaking. Most of the free field soil movement concentrated at the top two meters of depth, as a consequence of liquefaction in this area (Fig. 6). The bottom non-liquefiable sand layer behaved as a rigid body, and did not slide with respect to the bedrock base. The lower portion of the pile and soil domain deformed similarly. However, the maximum surface soil displacement is about 2.5 times that of the pile head. The relative movement of the pile head to the soil surface is about 28 cm at the end of the shaking, as also indicated in Fig. 7. The contour lines in the final deformed mesh (Fig. 9) clearly show the "flow" path of the liquefied soil near the pile head.

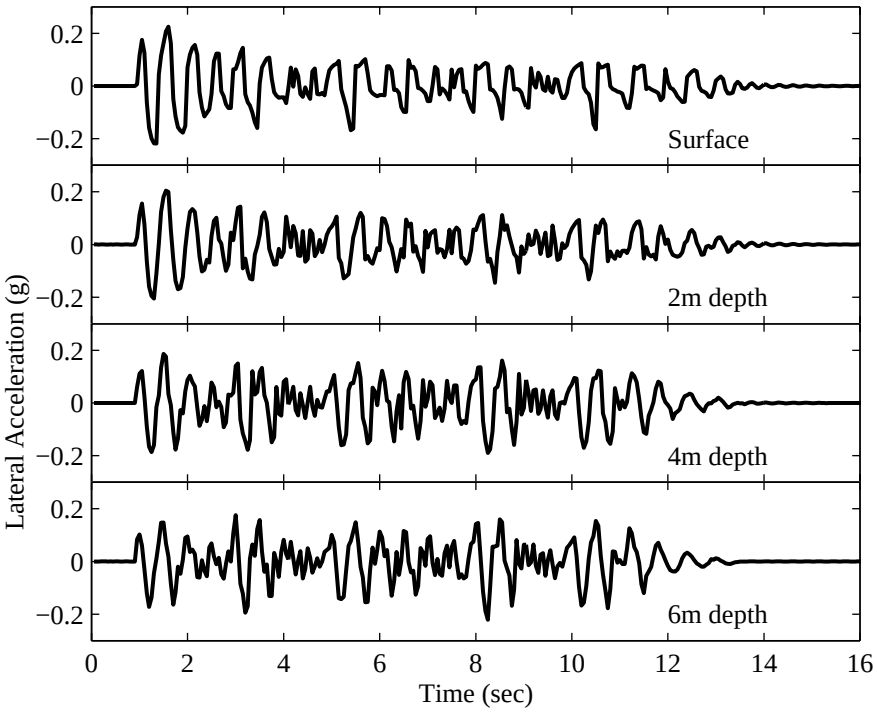

Fig. 5: Computed lateral acceleration time histories

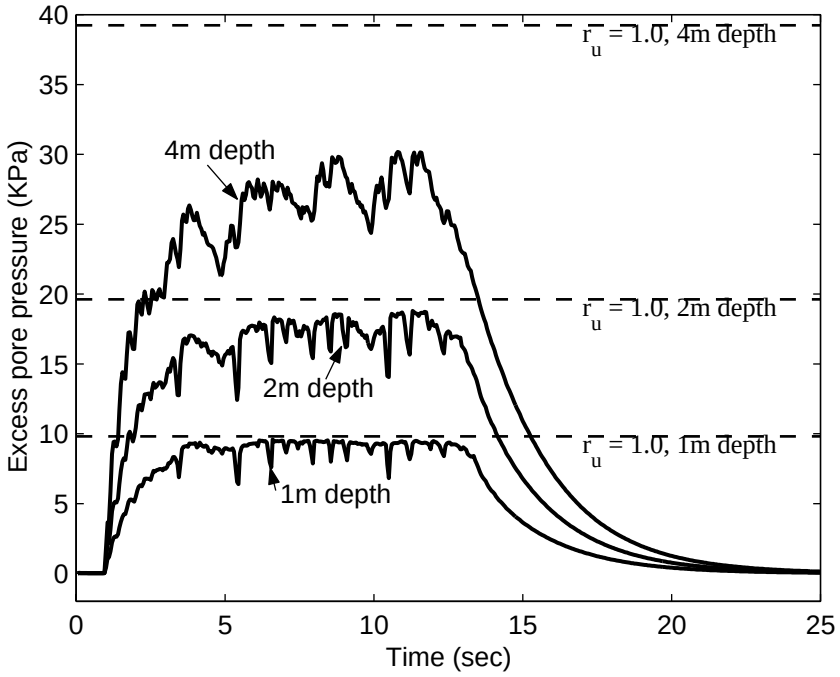

Fig. 6: Computed excess pore pressure time histories

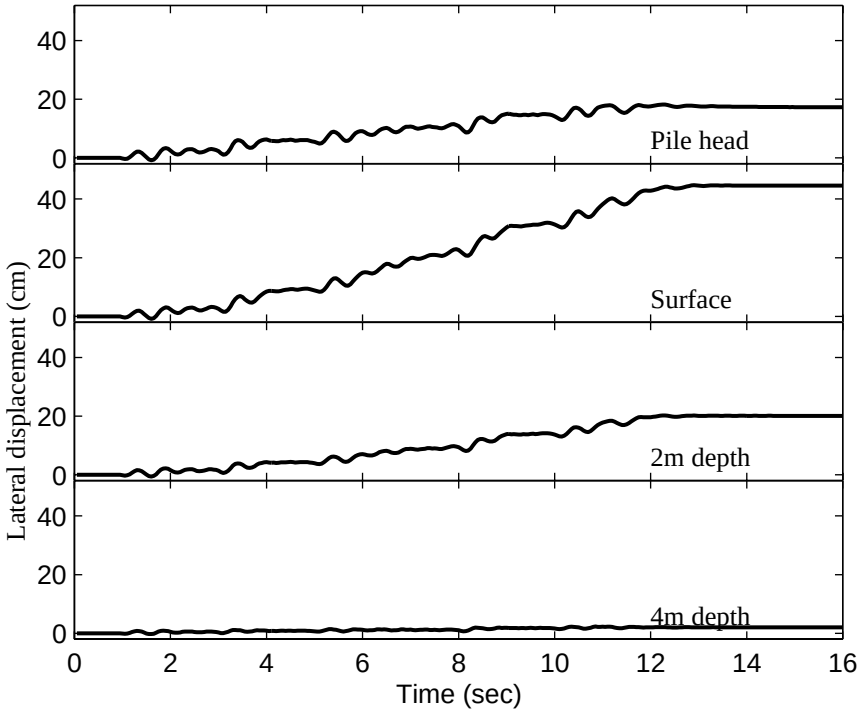

Fig. 7: Pile head and soil lateral displacement time histories

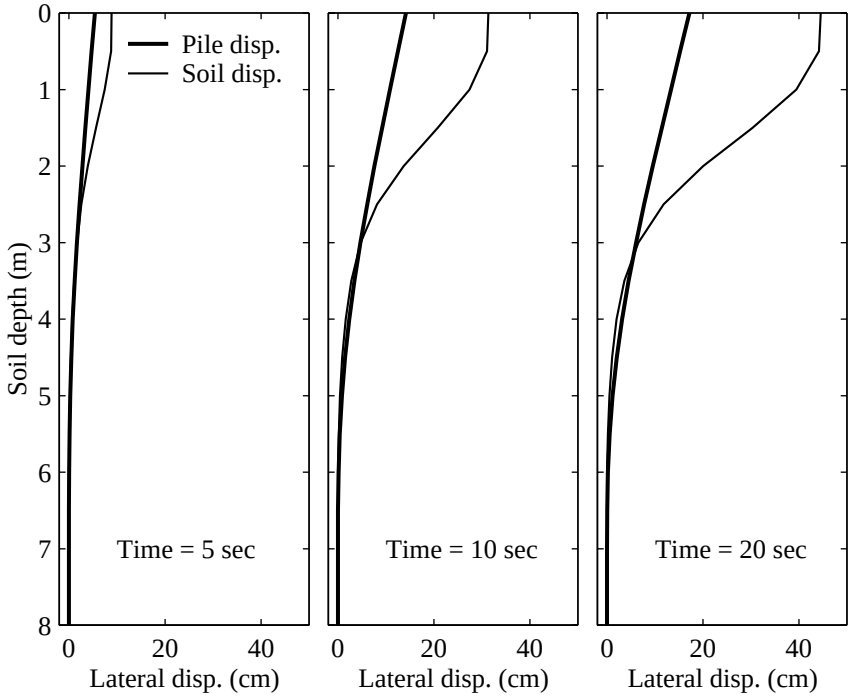

Fig. 8: Pile and free-field soil lateral displacement profiles at different time instants

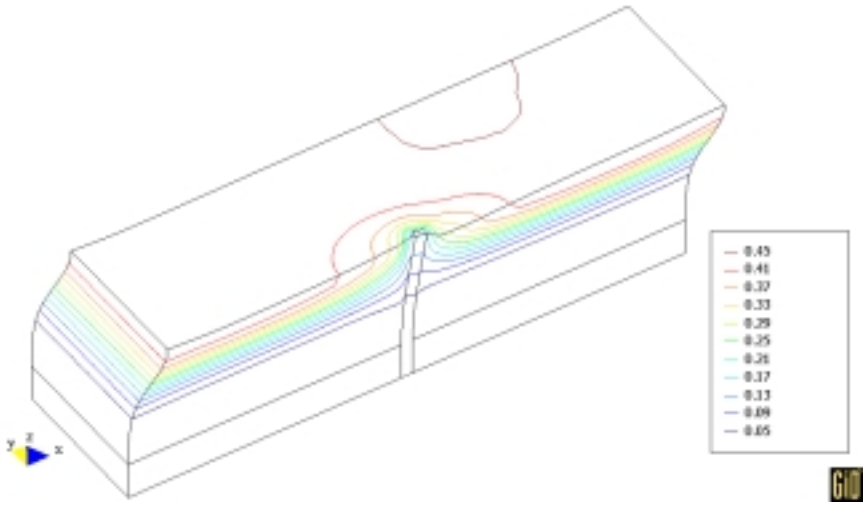

Fig. 9: Final deformed mesh (factor of 5) of the single pile foundation model (unit: m)

Pile Bending moment

Fig. 10 shows the bending moment time histories of the pile at different depths. The bending moment was obtained by integrating all vertical normal stresses from Gauss integration points across a section of the pile [32]. Gradual accumulation of permanent bending moment is particularly evident at 5.75m depth, a pattern similar to the lateral displacement accumulation in the soil and pile (Fig. 7). As indicated in the

bending moment profile (Fig. 11), the maximum moment (31kN-m) occurred at the interface of the two soil layers, at the end of the shaking.

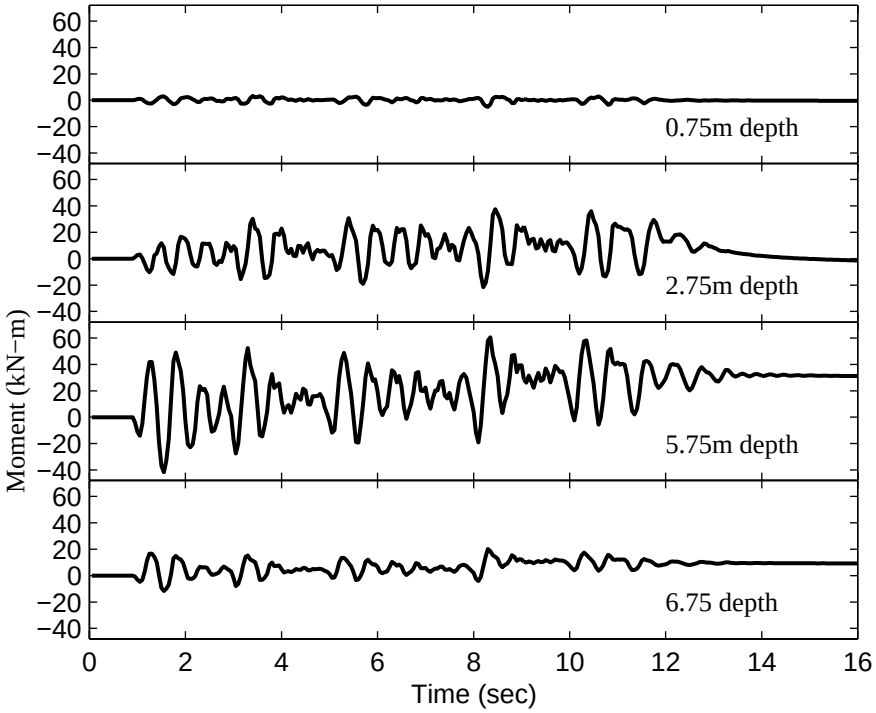

Fig. 10: Bending moment time histories

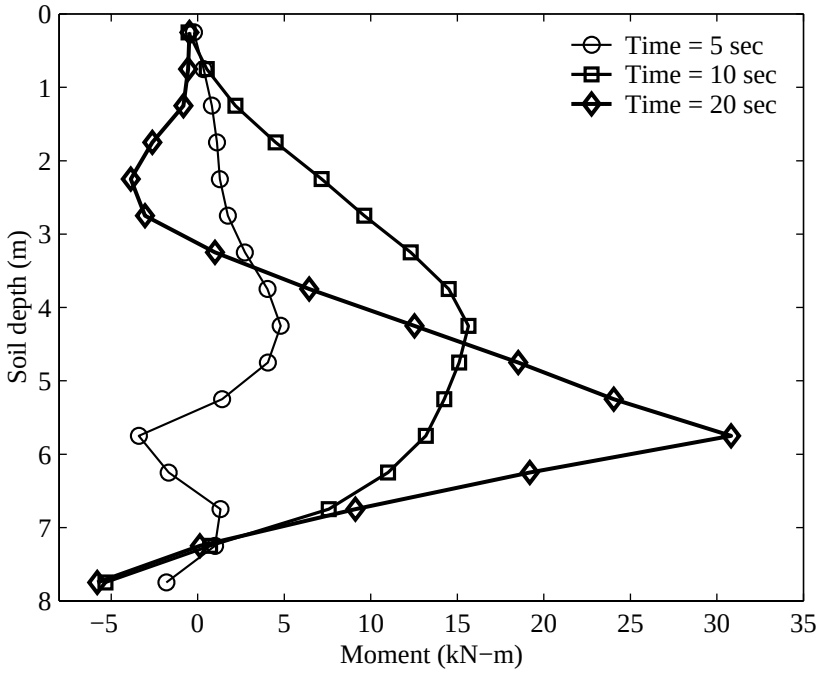

Fig. 11: Bending moment profiles at different times

SUMMARY AND CONCLUSIONS

A 3D high spatial resolution FE study of dynamic soil-pile interaction on parallel computers was presented in this paper. A new parallel nonlinear finite element program, ParCYCLIC, is employed to study this model. The computational results, including pore pressure generation/dissipation, soil lateral deformation during liquefaction, and pile displacement and bending moment, are presented and discussed. The study demonstrates the current capabilities of ParCYCLIC. Further development is underway to include beam element and high order solid element.

ACKNOWLEDGEMENTS

This research was supported by the National Science Foundation (NSF), Grants Number CMS-0084616, 0200510 and ANI-0205720 to University of California, San Diego, and Grant Number CMS-0084530 to Stanford University. This research was also supported by the Pacific Earthquake Engineering Research (PEER) Center, under the National Science Foundation Award Number EEC-9701568. Additional funding was also provided by the NSF cooperative agreement ACI-9619020 through computing resources provided by the National Partnership for Advanced Computational Infrastructure at the San Diego Supercomputer Center and the University of Michigan. This support is most appreciated.

REFERENCES

1. Mizuno H. "Pile damage during earthquakes in Japan (1923-1983)." in *Proc. Session on Dynamic Response of Pile Foundations*, T. Nogami, ed., ASCE, Atlantic City, April 27, 1987, pp. 53-77.

2. Matsui T, and Oda K. "Foundation damage of structures." *Soils and Foundations*, vol. Special Issue on Geotechnical Aspects of the January 17, 1995 Hyogoken-Nambu Earthquake, January, no., 1996, pp. 189-200.
3. Tokimatsu K, and Aska Y. "Effects of liquefaction-induced ground displacements on pile performance in the 1995 hyogoken-nambu earthquake." *Soils and Foundations*, vol. Special Issue on Geotechnical Aspects of the January 17, 1995 Hyogoken-Nambu Earthquake, No. 2, September, no., 1998, pp. 163-178.
4. Abdoun T. "Modeling of seismically induced lateral spreading of multi-layered soil and its effect on pile foundations," Ph.D. Thesis, Dept. of Civil Engineering, Rensselaer Polytechnic Institute, Troy, New York, 1997.
5. Yang Z, and Elgamal A. "Influence of permeability on liquefaction-induced shear deformation." *J. Engineering Mechanics*, vol. 128, no. 7, 2002, pp. 720-729, *ASCE*.
6. Parra E. "Numerical modeling of liquefaction and lateral ground deformation including cyclic mobility and dilation response in soil systems," Ph.D. Thesis, Dept. of Civil Engineering, Rensselaer Polytechnic Institute, Troy, NY, 1996.
7. Elgamal A, Yang Z, and Parra E. "Computational modeling of cyclic mobility and post-liquefaction site response." *Soil Dynamics and Earthquake Engineering*, vol. 22, no. 4, 2002, pp. 259-271.
8. Biot MA. "The mechanics of deformation and acoustic propagation in porous media." *Journal of Applied Physics*, vol. 33, no. 4, 1962, pp. 1482-1498.
9. Yang Z. "Numerical modeling of earthquake site response including dilation and liquefaction," Ph.D. Thesis, Dept. of Civil Engineering and Engineering Mechanics, Columbia University, New York, NY, 2000.
10. Chan AHC. "A unified finite element solution to static and dynamic problems in geomechanics," Ph.D. Dissertation, University of Wales, Swansea, U.K., 1988.
11. Zienkiewicz OC, Chan AHC, Pastor M, Paul DK, and Shiomi T. "Static and dynamic behavior of soils: A rational approach to quantitative solutions: I. Fully saturated problems." *Proceedings of the Royal Society London, Series A, Mathematical and Physical Sciences*, vol. 429, no., 1990, pp. 285-309.
12. Parra E, Adalier K, Elgamal A-W, Zeghal M, and Ragheb A. "Analyses and modeling of site liquefaction using centrifuge tests." in *Eleventh World Conference on Earthquake Engineering*, Acapulco, Mexico, June 23-28, 1996.
13. Elgamal A, Yang Z, Parra E, and Ragheb A. "Modeling of cyclic mobility in saturated cohesionless soils." *Int. J. Plasticity*, vol. 19, no. 6, 2003, pp. 883-905.
14. Yang Z, Elgamal A, and Parra E. "A computational model for cyclic mobility and associated shear deformation." *J. Geotechnical and Geoenvironmental Engineering*, vol. 129, no. 12, 2003, pp. 1119-1127, *ASCE*.
15. Prevost JH. "A simple plasticity theory for frictional cohesionless soils." *Soil Dynamics and Earthquake Engineering*, vol. 4, no. 1, 1985, pp. 9-17.
16. Elgamal A, Parra E, Yang Z, and Adalier K. "Numerical analysis of embankment foundation liquefaction countermeasures." *Journal of Earthquake Engineering*, vol. 6, no. 4, 2002, pp. 447-471.
17. Lacy S. "Numerical procedures for nonlinear transient analysis of two-phase soil system," Ph.D. Thesis, Princeton University, NJ, 1986.
18. Ishihara K, Tatsuoka F, and Yasuda S. "Undrained deformation and liquefaction of sand under cyclic stresses." *Soils and Foundations*, vol. 15, no. 1, 1975, pp. 29-44.
19. Arulmoli K, Muraleetharan KK, Hossain MM, and Fruth LS. "Velacs: Verification of liquefaction analyses by centrifuge studies, laboratory testing program, soil data report." *Report*, The Earth Technology Corporation, Project No. 90-0562, Irvine,CA, 1992.

20. Taboada VM. "Centrifuge modeling of earthquake-induced lateral spreading in sand using a laminar box," Ph.D. Thesis, Rensselaer Polytechnic Institute, Troy, NY, 1995.
21. Dobry R, Taboada V, and Liu L. "Centrifuge modeling of liquefaction effects during earthquakes." in *Proc. 1st Intl. Conf. On Earthquake Geotechnical Engineering, IS-Tokyo*, K. Ishihara, Balkema, Rotterdam, Tokyo, Japan, Nov. 14-16, 1995, pp. 1291-1324.
22. Law KH. "Large scale engineering computations on distributed memory parallel computers and distributed workstations." in *NSF Workshop on Scientific Supercomputing, Visualization and Animation in Geotechnical Earthquake Engineering and Engineering Seismology*, Carnegie-Mellon University, October, 1994.
23. Aluru NR. "Parallel and stabilized finite element methods for the hydrodynamic transport model of semiconductor devices," Ph.D. Thesis, Department of Civil and Environmental Engineering, Stanford University, Stanford, CA, 1995.
24. De Santiago E, and Law KH. "A distributed finite element method for solving the incompressible navier-stokes equations." *International Journal for Numerical Methods in Engineering*, vol. 39, no., 1996, pp. 4243-4258.
25. Law KH, and Mackay DR. "A parallel row-oriented sparse solution method for finite element structural analysis." *International Journal for Numerical Methods in Engineering*, vol. 36, no., 1993, pp. 2895-2919.
26. Mackay DR, Raefsky A, and Law KH. "An implementation of a generalized sparse/profile finite element solution method." *Computer and Structure*, vol. 41, no. 4, 1991, pp. 723-737.
27. Liu JWH. "A compact row storage scheme for cholesky factors using elimination tree." *ACM TOMS*, vol. 12, no., 1986, pp. 127.
28. Mackay DR. "Solution methods for static and dynamic structural analysis on distributed memory computers," Ph.D. Thesis, Department of Civil Engineering, Stanford University, 1992.
29. Peng J, Lu J, Law KH, and Elgamal A. "Parcyclic: Finite element modeling of earthquake liquefaction response on parallel computers." *Submitted to Int'J for Numerical and Analytical Methods in Geomechanics*, vol., no., 2004.
30. Lu J, Peng J, Elgamal A, Yang Z, and Law KH. "Parallel finite element modeling of earthquake liquefaction response." *Int'l Journal of Earthquake Engineering & Engineering Vibration*, vol. 3, no. 1, 2004, *in print*.
31. Abdoun T, and Dobry R. "Evaluation of pile foundation response to lateral spreading." *Soil Dynamics and Earthquake Engineering*, vol. 22, no. 9-12, 2002, pp. 1051-1058.
32. Yang Z. "Development of geotechnical capabilities into OpenSees platform and their applications in soil-foundation-structure interaction analyses," Ph.D. Thesis, Dept. of Civil Engineering, University of California, Davis, CA, 2002.